Journal of Informatics and Mathematical Sciences
Vol. 10, No. 3, pp. 443–454, 2018
ISSN 0975-5748 (online); 0974-875X (print)
Published by RGN Publications
DOI: 10.26713/jims.v10i3.788

http://www.rgnpublications.com

Research Article

Combined Effects of Magnetic Field and Slip Parameter on Hydromagnetic Flow Through Porous Media With Different Slip Velocities at Both the Porous Interface

K. Ramakrishnan

Department of Mathematics, Karpagam College of Engineering, Othakkal Mandapam, Coimbatore 641 032, Tamilnadu, India
krkresearch@gmail.com

Abstract. Effects of magnetic field and slip parameter on hydromagnetic flow through a uniform channel covered by porous media with different slip velocities at both the porous interface have been investigated. In the direction perpendicular to the motion of the fluid, a uniform magnetic field is applied. The analytical solution for the equations governing to the problem is obtained by using the Beavers-Joseph slip condition. Slip velocities at both the porous interface are assumed to be different. The flow characteristics such as axial velocity, slip velocity and the shear stress are calculated for different values of Hartmann number, porous parameter and slip parameter. It is observed that due to slip velocity variation in both the upper and lower walls, the distribution of flow pattern have altered.

Keywords. Magnetic field; Porous media; Different slip velocities and BJ slip condition

MSC. 76W05; 76S05

Received: January 18, 2018 **Accepted:** June 21, 2018

1. Introduction

The study of MHD flow through a porous medium in the presence of magnetic field spans a range of scientific and engineering domains, including earth science, life sciences and nuclear engineering. Several analytical and numerical works in the literature are devoted to the study of the MHD flow of a conducting fluid through a porous medium.

A classical approach to investigate the flow through or past porous media consists of solving the Navier-Stokes equations in the fluid medium and Darcy's equation in the porous medium. When we study transport problem in porous media, the essential part of the mathematical description is the correct specification of boundary conditions in the interface region.

Earlier, the existence of slip phenomenon at the boundaries and the interface has been observed in the flows of rarefied gases, hypersonic flows of chemically reacting binary mixture. Under certain conditions, researchers studied the slip phenomenon in the case of viscous incompressible fluid also. Beavers and Joseph [4] in their experimental work on boundary conditions at a naturally permeable wall, confirmed the existence of slip at the interface separating the flow in the channel and the permeable boundaries and developed the boundary condition known as BJ slip condition.

After the important work done by Beavers and Joseph, the problem of the interface region between a porous layer and a fluid-filled channel has received the most attention. Generally, simulation in the porous region can be modelled by either the Darcy or Brinkman or Brinkman-Forchheimer models. Importantly, the work of Neale and Nader [13] showed that for flow in a channel containing both fluid and porous regions, the Darcy model with the BJ condition gives the same solution as that obtained by using Brinkman model in which continuity of velocity and stress components are imposed at the interface. Later, many investigators (Vafai [18], Van Lankveld [19], Mikelic [12], Lebars and Worster [10], and Abuzaytoon *et al.* [1]) justified the use of BJ slip condition in the interface region where the transfer of momentum takes place.

In particular, two situations arise in the case of studies in flow through and past porous media: (i) In the presence of a solid boundary, there is a need to redefine permeability due to the increase in permeability near a solid wall. (ii) In flow over porous layers, there exists a permeability discontinuity at the interface between the flow regions. The above situations gave rise to the need for variable permeability models.

Stastna *et al.* [17] discussed the quasi-steady linear consolidation theory which is applied to a model brain under hydrodynamic loading and the role of a variable permeability in the analysis of the transient response. Hamdan and Kamel [7] analyzed the flow through variable permeability porous layers together with Brinkman's equation for the assumed configuration. Valentina Ciriello *et al.* [5] studied the influence of permeability varying to the flow direction on the spreading of plane porous gravity currents. Hansen *et al.* [8] presented a simple and highly accurate method to predict slip using equilibrium molecular dynamics method. Verma *et al.* [21] proposed a mathematical model for pulsatile flow of blood in a catheterized artery in presence of an axisymmetric stenosis with a velocity slip at the constricted wall.

A two-layered mathematical model of blood flow for a mild stenosis artery in the presence of axially variable, peripheral layer thickness and variable slip at the wall investigated by Harjeet Kumar *et al.* [9]. Rao and Agarwal [15] developed a theoretical model for the inclined slider bearing with porous layer attached to slider including slip parameter effects. In this case the upper and lower porous regions have different permeability parameters. Alharbi *et al.* [3] obtained exact solutions for the flow variables involved in the flow through a porous medium with variable permeability. Gaur *et al.* [6] studied the effects of variable permeability on an MHD magneto polar fluid past a vertical plate in the slip flow regime.

Numerous of research works have been carried out in the case of flow through porous media with same/different slip velocities at the porous interface (Makinde and Osalusi [11], Ramakrishnan and Shailendhra [14], Venna [20], Zhao *et al.* [22], Abuzaytoon *et al.* [2], and Shu *et al.* [16]).

In the present work, effects of Hartmann number and slip parameter on hydromagnetic flow through a uniform channel covered by porous media with different slip velocities at both the porous interface have been investigated. A uniform magnetic field is applied in the direction perpendicular to the motion of the fluid. The analytical solution for the equations governing to the problem is obtained using the BJ slip condition. In both the porous interface, slip velocities are assumed to be different.

2. Formulation of the Problem

To study the behaviour of variable permeability in the lower and upper porous walls in the case of hydromagnetic flow through uniform porous channel, consider the physical configuration as shown in Figure 1.

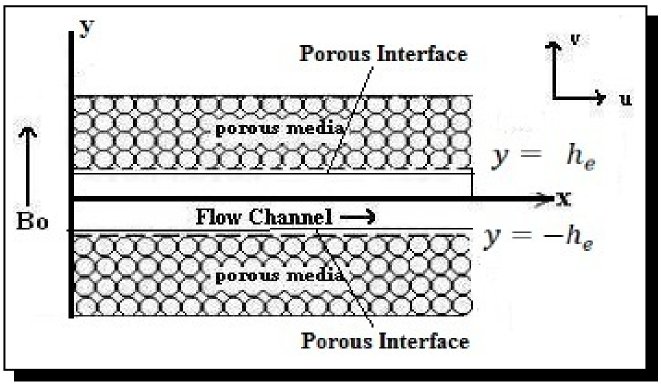

Figure 1. Physical Model

A long uniform porous channel bounded by porous walls where the bounding surface on either side represented by the lines $y = \pm h_e$ is taken. The nature of the fluid assumed to be laminar, steady, viscous and Newtonian with constant density ρ, viscosity μ and small electrical conductivity σ_e. It is also assumed that the channel is symmetrical about the x-axis. The porous layer is assumed to be homogeneous, isotropic and densely packed. In the direction perpendicular to the motion of the fluid, a uniform magnetic field H_0 is applied. $B_0 = \mu_e H_0$ is the electromagnetic induction and μ_e is the magnetic permeability. Further, it is assumed that the upper and lower porous walls have different permeability. Since, the channel is infinite in length, all the physical quantities (except pressure) depend only on y. Under these assumptions after neglecting the inertia effects, the equations governing to the problem are

$$\frac{\partial^2 u}{\partial y^2} - \frac{\sigma_e B_0^2}{\mu} u = \frac{1}{\mu}\frac{\partial p}{\partial x}, \tag{1}$$

$$\frac{1}{\mu}\frac{\partial}{\partial y}\left(p + \frac{1}{2}B_x^2\right) = 0, \tag{2}$$

$$v = 0 \tag{3}$$

and those in the porous layer are governed by Darcy Velocity,

$$Q_x = -\frac{k}{\mu}\frac{\partial p}{\partial x} \quad \text{and} \quad Q_y = -\frac{k}{\mu}\frac{\partial p}{\partial y}, \tag{4}$$

where u and v are the velocity components in the x and y direction. Note that the equation of continuity $\nabla \cdot \vec{q} = 0$ gives $v = 0$.

The boundary conditions are,

$$\frac{du}{dy} = \bar{\alpha}\left(\frac{u_{B1} - Q_1}{\sqrt{k_1}}\right) \quad \text{at } y = -h_e, \tag{5}$$

$$\frac{du}{dy} = -\bar{\alpha}\left(\frac{u_{B2} - Q_2}{\sqrt{k_2}}\right) \quad \text{at } y = h_e, \tag{6}$$

$$\int_{-1}^{1} u(y)dy = n_f, \tag{7}$$

$$u = u_{B1} \quad \text{at } y = -h_e, \tag{8}$$

$$u = u_{B2} \quad \text{at } y = h_e \tag{9}$$

and

$$Q_1 = -\frac{k_1}{\mu}\frac{\partial p}{\partial x} \quad \text{and} \quad Q_2 = -\frac{k_2}{\mu}\frac{\partial p}{\partial x}, \tag{10}$$

where n_f is the net flux through the channel, u_{B1} and u_{B2} are the slip velocities, k_1 and k_2 are the permeability of the porous material in the Lower wall and Upper wall respectively and $\bar{\alpha}$ is the dimensionless constant, called slip parameter. Here, $\sigma_1 = \frac{h_e}{\sqrt{k_1}}$ and $\sigma_2 = \frac{h_e}{\sqrt{k_2}}$ are the porous parameter in the lower and upper walls, respectively. The conditions (5) and (6) are the BJ slip conditions.

3. Solution of the Problem

In the case of uniform channel flow, one can use the approximation that the wall slope is everywhere negligible (Ramakrishnan and Shailendhra [14]). Introduce the transform quantity $y = \xi h_e$ in eqns. (1)–(3) and eliminating the pressure term, we have

$$\frac{d^3 u}{d\xi^3} - M^2\frac{du}{d\xi} = 0, \tag{11}$$

where $M^2 = \frac{B_0^2 h^2 \sigma_e}{\mu}$ is the square of the Hartmann number.

The conditions (5) to (7) changes under the transformation $y = \xi h_e$ as follows:

$$\frac{du}{d\xi} = \bar{\alpha}\sigma_1(u_{B1} - Q_1) \quad \text{at } \xi = -1, \tag{12}$$

$$\frac{du}{d\xi} = -\bar{\alpha}\sigma_2(u_{B2} - Q_2) \quad \text{at } \xi = 1, \tag{13}$$

$$\int_{-1}^{1} u(\xi)d\xi = \frac{n_f}{h_e} = N_F\,. \tag{14}$$

Solving eqn. (11) subject to the conditions (12) to (14), we have

$$u(\xi) = \frac{N_F}{2} + \frac{\bar{\alpha}}{2M}\left[\frac{\sigma_1(u_{B1} - Q_1) - \sigma_2(u_{B2} - Q_2)}{\cosh(M)}\right]\sinh(M\xi) + \frac{\bar{\alpha}}{2M^2}[\sigma_1(u_{B1} - Q_1) + \sigma_2(u_{B2} - Q_2)]\left[\frac{\sinh(M) - M\cosh(M\xi)}{\sinh(M)}\right], \tag{15}$$

$$u_{B1} = \frac{\frac{N_F}{2}(\eta_5 + \eta_3) - (\eta_4\eta_5 + \eta_3\eta_7)}{\eta_2\eta_5 - \eta_3\eta_6}, \tag{16}$$

$$u_{B2} = \frac{\frac{N_F}{2}(\eta_2 + \eta_6) - (\eta_2\eta_7 + \eta_4\eta_6)}{\eta_2\eta_5 - \eta_3\eta_6}, \tag{17}$$

$$N_F = \frac{2\eta_{10} + \bar{\alpha}\left(\frac{1}{\sigma_1} + \frac{1}{\sigma_2}\right)\eta_{10} + 2\bar{\alpha}(\sigma_1\eta_{11} + \sigma_2\eta_{12})}{\bar{\alpha}\left[\eta_{13} + \frac{M^2}{\bar{\alpha}}\eta_{10}\right]}\left(-R\frac{\partial p}{\partial x}\right), \tag{18}$$

where

$$\eta_1 = \frac{\sinh(M) - M\cosh(M)}{\sinh(M)}, \qquad \chi_1 = \eta_1 - M\tanh(M),$$

$$\chi_2 = \eta_1 + M\tanh(M), \qquad \eta_2 = 1 - \frac{\bar{\alpha}\sigma_1\chi_1}{2M^2},$$

$$\eta_3 = \frac{\bar{\alpha}\sigma_2\chi_2}{2M^2}, \qquad \eta_4 = \frac{\bar{\alpha}}{2M^2}[\sigma_1Q_1\chi_1 + \sigma_2Q_2\chi_2],$$

$$\eta_5 = 1 - \frac{\bar{\alpha}\sigma_2\chi_1}{2M^2}, \qquad \eta_6 = \frac{\bar{\alpha}\sigma_1\chi_2}{2M^2},$$

$$\eta_7 = \frac{\bar{\alpha}}{2M^2}[\sigma_1Q_1\chi_2 + \sigma_2Q_2\chi_1], \qquad \eta_8 = \frac{\bar{\alpha}}{2M^2}\left[\frac{1}{\sigma_1}\chi_1 + \frac{1}{\sigma_2}\chi_2\right],$$

$$\eta_9 = \frac{\bar{\alpha}}{2M^2}\left[\frac{1}{\sigma_1}\chi_2 + \frac{1}{\sigma_2}\chi_1\right], \qquad \eta_{10} = \eta_2\eta_5 - \eta_3\eta_6,$$

$$\eta_{11} = \eta_5\eta_8 + \eta_3\eta_9, \qquad \eta_{12} = \eta_2\eta_9 + \eta_6\eta_8.$$

When both the lower and upper walls have the same permeability, the above results reduced to those in the case of Hydromagnetic flow through a uniform channel bounded by porous media (Ramakrishnan and Shailendhra [14]).

4. Results and Discussion

The purpose of the present discussion is to study the combined effects of Hartmann number (M), slip parameter ($\bar{\alpha}$) and porous parameter (σ) on the axial velocity ($u(\xi)$), slip velocities (u_{B_1} and u_{B_2}) and shear stress (τ_{xy}) on hydromagnetic flow through porous media with different slip velocities at both the porous interface. The effects of various parameters on the axial velocity are discussed with the help of graphs and those on the slip velocity and shear stress are done with the help of tables.

To understand the influence of different slip velocities at both the porous interface, initially varying the values of porous parameter (σ_2) in the upper wall by taking $\sigma_2 = 10^2, 10^3, 10^4$. Here, the value of porous parameter in the lower wall is fixed as $\sigma_1 = 10^1$ (presence of Darcy velocity $Q_1 = 0.01$). In this case, the distribution of axial velocity is depicted in Figures. 2–5. From Figure 2 and 3, it is clear that the pattern of axial velocity profile is parabola. These figures show that by increasing the Hartmann number M, the axial velocity decreases. It is noticed that a maximum peak occurs in the central line of the channel when $M = 1.0$, which flattens as M is increased. Thus, it is seen that the presence of magnetic field slows down the flow motion of the fluid, confirming the fact that the magnetic field brings in rigidity in conducting fluids.

From Figure 2 and 3, it is noticed that the porous parameter have generally a retarding effect on the axial velocity which indicates the fact that the effect of porosity is to reduce the flow. However, from Figure 2 it is observed that for $M \geq 4$, increase of σ_2 in the upper wall results in increase of axial velocity in the central portion of the channel. This is due to variation in permeability at both the porous interface. But from Figure 3, it is noticed that for $M \geq 4$, increase of σ_2 have no significant effect on axial velocity. In this case the upper wall behaves almost like an impermeable wall. Again from Figures 2 and 3, it is seen that for higher values of the Hartmann number ($M \geq 6$), the flow is reversed significantly in the vicinity of upper wall than in the lower wall. Comparing Figure 2 and 3, it is clear that increase of slip parameter ($\bar{\alpha}$) results in decrease of axial velocity.

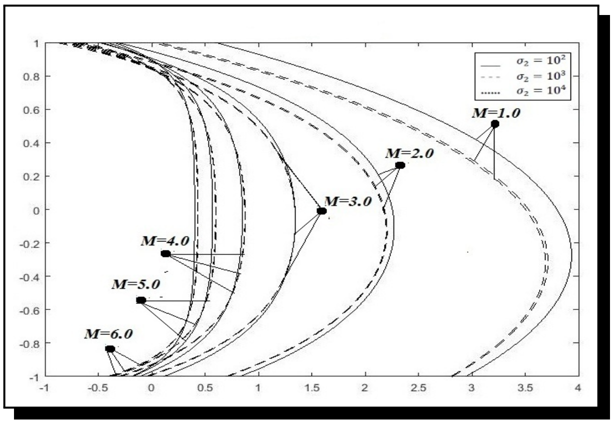

Figure 2. Axial velocity, $u(\xi)$ for $\bar{\alpha} = 0.1$ and $\sigma_1 = 10^1$ and different values of M

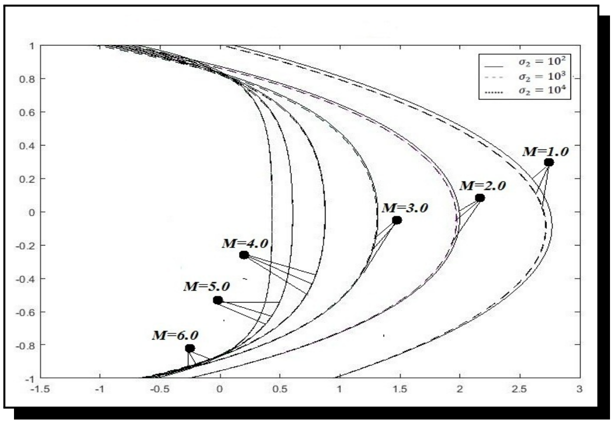

Figure 3. Axial velocity, $u(\xi)$ for $\bar{\alpha} = 0.5$ and $\sigma_1 = 10^1$ and different values of M

From Figure 4 and 5, it is observed that both the porous parameter and slip parameter reduce the axial velocity in the absence of magnetic field. Comparing Figures 2 to 5, it is noticed that the value of axial velocity is more near the lower wall than in the upper wall due to the permeable factor present in the lower wall and it induces a slip near the lower wall. It is also noticed that when $\sigma_1 = 10^6$ (absence of Darcy velocity, $Q_1 = 0$) the axial velocity distribution in the upper wall is dominated (not shown), since in this case lower wall behaves like an impermeable wall.

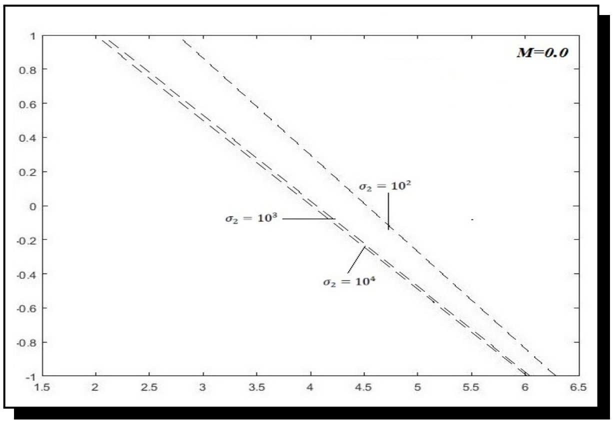

Figure 4. Axial velocity, $u(\xi)$ for $\bar{\alpha} = 0.1$ and $\sigma_1 = 10^1$ and $M = 0$

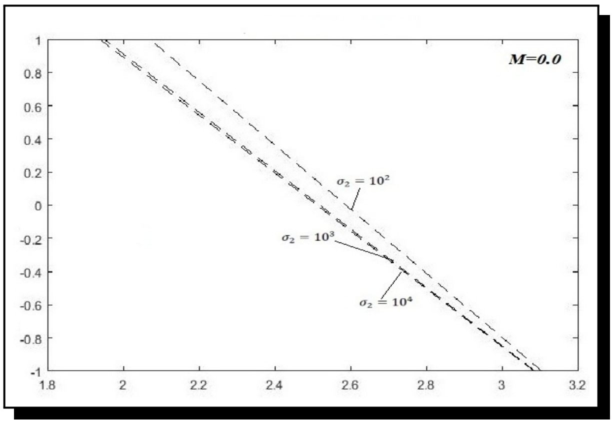

Figure 5. Axial velocity, $u(\xi)$ for $\bar{\alpha} = 0.5$ and $\sigma_1 = 10^1$ and $M = 0$

Figures 6–9, illustrate the distribution of axial velocity when lower wall given different porous parameter values. In the lower wall, the values of porous parameter (σ_1) are assumed to be $\sigma_1 = 10^2, 10^3, 10^4$ and the porous parameter in the upper wall is fixed as $\sigma_2 = 10^1$ (presence of Darcy velocity, $Q_2 = 0.01$). Figure 6 and 7 show that the magnetic field and Porosity decrease the axial velocity. It is also seen that the reversal of flow is more significant near the lower wall than in the case of upper wall. For large value of porous parameter ($\sigma_1 \geq 10^6$) there is no significant change in the axial velocity (not shown) which indicates that in this case the lower wall behaves like an impermeable wall. Figure 8 and 9, it is observed that the porous parameter and slip parameter have decrease the axial velocity in the absence of magnetic field. Comparing Figures 6 to 9, it is observed that the value of axial velocity is more near the upper wall than in the lower wall due to the slip factor present in the upper wall.

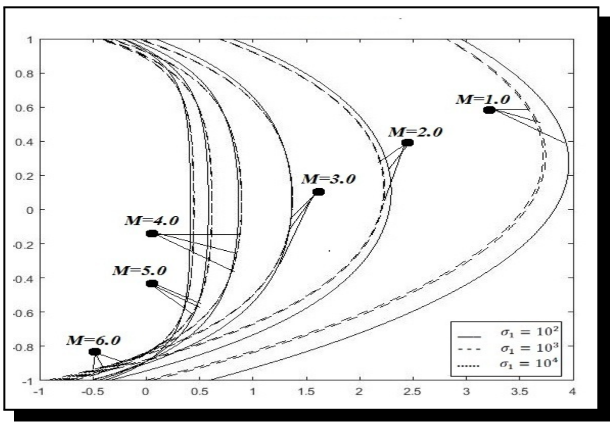

Figure 6. Axial velocity, $u(\xi)$ for $\bar{\alpha} = 0.1$ and $\sigma_2 = 10^1$ and different values of M

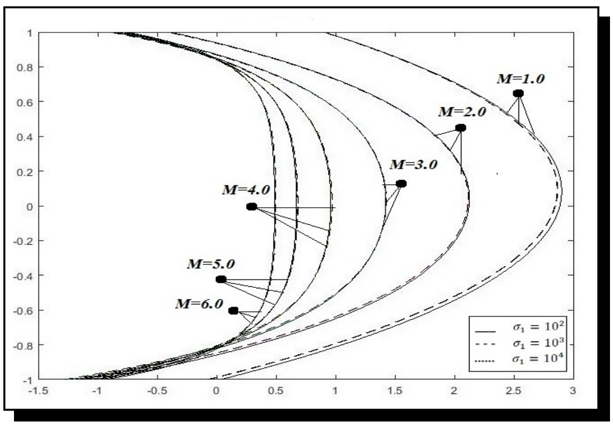

Figure 7. Axial velocity, $u(\xi)$ for $\bar{\alpha} = 0.5$ and $\sigma_2 = 10^1$ and different values of M

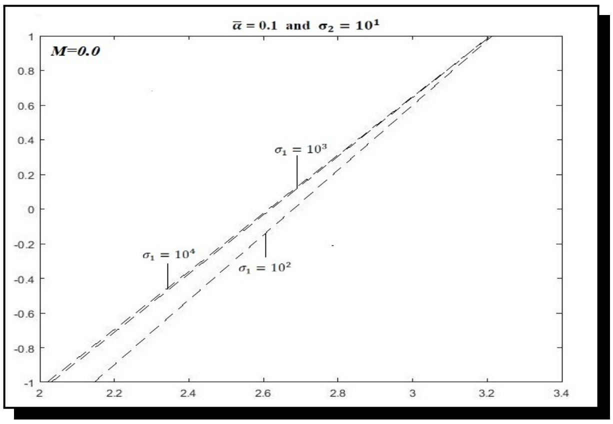

Figure 8. Axial velocity, $u(\xi)$ for $\bar{\alpha} = 0.1$ and $\sigma_2 = 10^1$ and $M = 0$

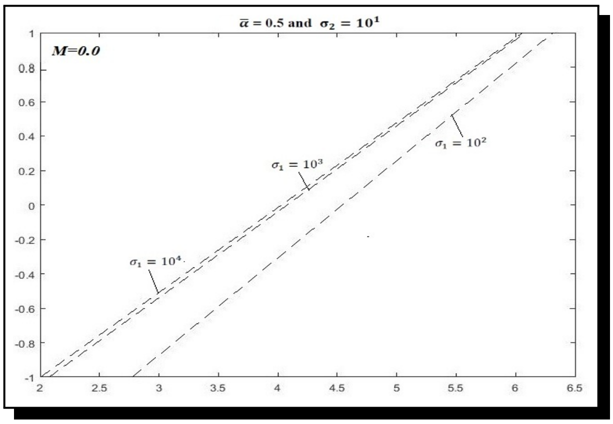

Figure 9. Axial velocity, $u(\xi)$ for $\bar{\alpha} = 0.5$ and $\sigma_2 = 10^1$ and $M = 0$

Distribution of slip velocity for different values of porous parameter (σ_1 and σ_2), slip parameter ($\bar{\alpha}$) and Hartmann number(M) is shown in Tables 1–4.

Table 1. Distribution of Slip Velocity in the Lower and Upper walls ($\bar{\alpha} = 0.1$ and $\sigma_1 = 10^1$)

$\sigma_2 \rightarrow$ / $M \downarrow$	10^2	10^4	10^6	$\sigma_2 \rightarrow$ / $M \downarrow$	10^2	10^4	10^6
0.0	4.2990	4.0387	4.0360	0.0	0.7735	0.0080	7.9×10^{-5}
2.0	1.5341	1.4769	1.4762	2.0	0.3832	0.0044	4.4×10^{-5}
4.0	0.5562	0.5382	0.5379	4.0	0.1923	0.0026	2.6×10^{-5}
6.0	0.2820	0.2735	0.2734	6.0	0.1177	0.0018	1.8×10^{-5}

Table 2. Distribution of Slip Velocity in the Lower and Upper walls ($\bar{\alpha} = 0.5$ and $\sigma_1 = 10^1$)

$\sigma_2 \rightarrow$ / $M \downarrow$	10^2	10^4	10^6	$\sigma_2 \rightarrow$ / $M \downarrow$	10^2	10^4	10^6
0.0	1.1623	1.1478	1.1476	0.0	0.1279	0.0013	1.3×10^{-5}
2.0	0.6433	0.6369	0.6369	2.0	0.0788	0.0008	0.8×10^{-6}
4.0	0.3285	0.3252	0.3251	4.0	0.0464	0.0004	0.5×10^{-6}
6.0	0.2041	0.2019	0.2019	6.0	0.0321	0.0003	0.3×10^{-6}

Table 3. Distribution of Slip Velocity in the Lower and Upper walls ($\bar{\alpha} = 0.1$ and $\sigma_2 = 10^1$)

$\sigma_1 \rightarrow$ / $M \downarrow$	10^2	10^4	10^6	$\sigma_1 \rightarrow$ / $M \downarrow$	10^2	10^4	10^6
0.0	0.7771	0.0080	8.0×10^{-5}	0.0	4.3191	4.0627	4.0601
2.0	0.3854	0.0045	4.5×10^{-5}	2.0	1.5428	1.4881	1.4874
4.0	0.1934	0.0026	2.6×10^{-5}	4.0	0.5594	0.5428	0.5425
6.0	0.1184	0.0018	1.8×10^{-5}	6.0	0.2834	0.2759	0.2758

Table 4. Distribution of Slip Velocity in the Lower and Upper walls ($\bar{a} = 0.5$ and $\sigma_2 = 10^1$)

$\sigma_1 \rightarrow$ / $M \downarrow$	10^2	10^4	10^6	$\sigma_1 \rightarrow$ / $M \downarrow$	10^2	10^4	10^6
0.0	0.1325	0.0013	1.3×10^{-5}	0.0	1.2011	1.1916	1.1915
2.0	0.0818	0.0008	0.8×10^{-6}	2.0	0.6659	0.6625	0.6625
4.0	0.0483	0.0005	0.5×10^{-6}	4.0	0.3397	0.3381	0.3381
6.0	0.0333	0.0004	0.4×10^{-6}	6.0	0.2106	0.2096	0.2096

From Tables 1–4, it is generally observed that slip velocity decreases when the Hartmann number (M) is increased. Table 1 and 2 show that increase in porous parameter reduce the slip velocity in both the lower and upper walls. It is also noticed that when increase of σ_2 from 10^2 to 10^6 and for fixed value of $\sigma_1 = 10$, results in decrease of slip velocity gradually in the lower wall and rapidly in the upper wall. For $\sigma_2 = 10^6$, from Table 1 and 2 indicate that slip velocity is vanish in the upper wall for all possible values of M. As mentioned above, in this case the upper wall becomes impermeable. On the other hand from Table 3 and 4, it is clear that increase of σ_1 in the lower wall rapidly make the lower permeable wall into impermeable. Comparing Table 1–4, show that the effect of slip parameter ($\bar{a}$) is to decrease the slip velocity at both the walls.

Distribution of shear stress for different values of porous parameter (σ_1 and σ_2), slip parameter ($\bar{a}$) and Hartmann number(M) is presented in Table 5–8. From Table 5– 8, it is clear that the effect of Hartmann number (M) is to reduce the stress for all possible values of the other parameters. Also from Table 5– 8, it is observed that the values of shear stress in the lower wall are positive and in the upper wall are negative. This indicate the fact that the stress acts from the lower wall in the upward direction and it acts in the doward direction from the upper wall.

Table 5. Distribution of Shear Stress in the Lower and Upper walls ($\bar{a} = 0.1$ and $\sigma_1 = 10^1$)

$\sigma_2 \rightarrow$ / $M \downarrow$	10^2	10^4	10^6	$\sigma_2 \rightarrow$ / $M \downarrow$	10^2	10^4	10^6
0.0	4.1990	3.9387	3.9360	0.0	−7.7245	−7.9695	−7.9720
2.0	1.4341	1.3769	1.3762	2.0	−3.8219	−4.4316	−4.4387
4.0	0.4562	0.4382	0.4379	4.0	−1.9129	−2.5820	−2.5910
6.0	0.1820	0.1735	0.1734	6.0	−1.1674	−1.8037	−1.8135

Table 6. Distribution of Shear Stress in the Lower and Upper walls ($\bar{a} = 0.5$ and $\sigma_1 = 10^1$)

$\sigma_2 \rightarrow$ / $M \downarrow$	10^2	10^4	10^6	$\sigma_2 \rightarrow$ / $M \downarrow$	10^2	10^4	10^6
0.0	5.3117	5.2390	5.2382	0.0	−6.3461	−6.3855	−6.3859
2.0	2.7167	2.6846	2.6843	2.0	−3.8880	−4.0044	−4.0056
4.0	1.1425	1.1259	1.1257	4.0	−2.2715	−2.4256	−2.4272
6.0	0.5204	0.5097	0.5096	6.0	−1.5526	−1.7192	−1.7210

Table 5 and 6 indicate that when σ_2 varying from 10^2 to 10^6 and fixed $\sigma_1 = 10^1$, the values of shear stress in the lower wall decrease whereas in the upper wall increases numerically. It is noticed that for $\sigma_2 \geq 10^8$ (absence of Darcy velocity, i.e., $Q_2 = 0$), the value of shear stress in the upper wall become constant. It shows clearly that the value of shear stress is more in the case of impermeable wall than that of permeable wall.

Table 7. Distribution of Shear Stress in the Lower and Upper walls ($\bar{\alpha} = 0.1$ and $\sigma_2 = 10^1$)

$\sigma_1 \rightarrow$ / $M \downarrow$	10^2	10^4	10^6	$\sigma_1 \rightarrow$ / $M \downarrow$	10^2	10^4	10^6
0.0	7.7610	8.0174	8.0200	0.0	−4.2191	−3.9627	−3.9601
2.0	3.8439	4.4660	4.4732	2.0	−1.4428	−1.3881	−1.3874
4.0	1.9241	2.6048	2.6140	4.0	−0.4594	−0.4428	−0.4425
6.0	1.1738	1.8203	1.8303	6.0	−0.1834	−0.1759	−0.1758

Table 8. Distribution of Shear Stress in the Lower and Upper walls ($\bar{\alpha} = 0.5$ and $\sigma_2 = 10^1$)

$\sigma_1 \rightarrow$ / $M \downarrow$	10^2	10^4	10^6	$\sigma_1 \rightarrow$ / $M \downarrow$	10^2	10^4	10^6
0.0	6.5739	6.6481	6.6488	0.0	−5.5053	−5.4579	−5.4574
2.0	4.0410	4.1853	4.1866	2.0	−2.8293	−2.8126	−2.8124
4.0	2.3648	2.5418	2.5435	4.0	−1.1984	−1.1905	−1.1904
6.0	1.6162	1.8035	1.8054	6.0	−0.5528	−0.5480	−0.5480

Table 7 and 8 show that when σ_1 varying from 10^2 to 10^6 and fixed $\sigma_2 = 10^1$, the values of shear stress in the upper wall decrease in magnitude whereas in the lower wall increases. It is noticed that for $\sigma_1 \geq 10^8$ (absence of Darcy velocity, i.e., $Q_1 = 0$), the value of shear stress in the lower wall become constant.

Comparing Table 5–8, it is evident that increase of slip parameter ($\bar{\alpha}$) from 0.1 to 0.5 reduce the shear stress numerically at varying permeable wall whereas it increase numerically the shear stress at fixed permeable wall. It is also observed that when porous parameter and slip parameter assumed its maximum value, its effect on shear stress is insignificant.

5. Conclusion

Combined effects of porous parameter, Hartmann number and slip parameter on the hydromagnetic flow through a uniform channel covered by porous media with different slip velocities at both the porous interface is investigated. The results showed that the axial velocity of the fluid is reduced by porous parameter, Hartmann number and slip parameter. It is also observed the reversal of flow near the upper/lower walls due to the change in slip velocity at both the walls. The distribution of Shear stress at both the walls showed an increasing/decreasing trend depending on wall permeable factor. By the proper choice of values of flow parameters, one can have control over the flow field.

Competing Interests

The author declares that he has no competing interests.

Authors' Contributions

The author wrote, read and approved the final manuscript.

References

[1] M.S. Abuzaytoon and M.H. Hamdan, A note on the beavers and Joseph condition for flow over a Forchheimer porous layer, *International Journal of Research in Engineering and Science* **5**(3) (2017), 13 – 20.

[2] M.S. Abuzaytoon, T.L. Alderson and M.H. Hamdan, Flow over a Darcy porous layer of variable permeability, *Journal of Applied Mathematics and Physics* **14** (2016), 86 – 99, DOI: 10.4236/jamp.2016.41013.

[3] S.O. Alharbi, T.L. Alderson and M.H. Hamdan, Exact solution of fluid flow through porous media with variable permeability for a given vorticity distribution International Journal of Enhanced Research in Science, *Technology and Engineering* **5**(5) (2016), 262 – 276.

[4] G.S. Beavers and D.D. Joseph, Boundary conditions at a naturally permeable wall, *J. Fluid Mech.* **30** (Part-I) (1967), 197 – 207, DOI: 10.1017/s002211206.

[5] V. Ciriello, V. Di Federico, R. Archetti and S. Longo, Effect of variable permeability on the propagation of thin gravity currents in porous media, *International Journal of Non-Linear Mechanics* **57** (2013), 168 – 175, DOI: 10.1016/j.ijrnonlinmec2013.07.003.

[6] P.K. Gaur, A.K. Jha and R. Sharma, Magneto-Polar fluid flow through a Porous medium of variable permeability in slip flow regime, *Int. J. Applied Mechanics and Engineering* **21**(2) (2016), 323 – 339, DOI: 10.1515/ijame-2016.0020.

[7] M.H. Hamdan and M.T. Kamel, Flow through variable permeability porous layers, *Adv. Theor. Appl. Mech.* **4**(3) (2011), 135 – 145.

[8] J.S. Hansen, B.D. Todd and P.J. Daivis, Prediction of fluid velocity slip at solid surfaces, *Physical Review E* **84** (2011), 1 – 8, DOI: 10.1103/PhysRevE.84.016313.

[9] R.S. Harjeet Kumar, C.S. Kumar and S. Kumar, A mathematical model for different shapes of stenosis and slip velocity at the wall through mild stenosis artery, *Advances in Applied Mathematical Bio Sciences* **5**(1) (2014), 9 – 18.

[10] M. Lebars and M.G. Worster, Interfacial conditions between a pure fluid and a porous medium: implications for binary alloy solidification, *J. Fluid Mech.* **550** (2006), 149 – 173, DOI: 10.1017/s0022/12005007998.

[11] O.D. Makinde and E. Osalusi, MHD flow in a channel with slip at the permeable boundaries, *Rom. J. Phys.* **51**(3) (2006), 319 – 328.

[12] A. Mikelic, On the effect boundary conditions between different flow regions, *Proceedings of first Conference on Applied Mathematics and Computation*, Dubrovnik, Croatia, September 13-18, pp. 21-37 (1999).

[13] G. Neale and W. Nader, Practical significance of Brinkman's extension of Darcy's law: coupled parallel flows within a channel and a bounding porous medium, *The Can. J. Chem. Eng.* **52** (1974), 475 – 478, DOI: 10.1002/cjce.5450520407.

[14] K. Ramakrishnan and K. Shailendhra, Hydromagnetic flow through uniform channel bounded by porous media, *Appl. Math. Mech.-Engl. Ed.* **32**(7) (2011), 837 – 846, DOI: 10.1007/s/0483-011-1463-7.

[15] P.S. Rao and S. Agarwal, Effect of permeability and different slip velocities at both the porous interface using couple stress fluids on the slider bearing load carrying mechanism, *Proceedings of the institution of Mechanical Engineers, Part J: Journal of Engineering Tribology* **230**(2) (2016), 196 – 201, DOI: 10.1177/1350650115595054.

[16] J.-J. Shu, J.B.M. Teo and W.K. Chan, Fluid velocity slip and temperature jump at a solid surface, *Applied Mechanics Reviews* **69**(2) (2017), 1 – 32, DOI: 10.1115/1.4036191.

[17] M. Stastna, G. Tenti, S. Sivaloganathan and J.M. Drake, Brain bio mechanics: consolidation theory of hydrocephalus variable permeability and transient effects, *Canadian Applied Mathematics Quarterly* **7**(1) (1999), 93 – 109.

[18] K. Vafai, Fluid mechanics of the interface region between a porous medium and a fluid layer - An exact solution, *Int. J. Heat Fluid Flow* **11**(3) (1990), 254 – 256, DOI: 10.1016/0142-727X(90)90045-D.

[19] M.A.M. Van Lankveld, Validation of boundary conditions between a porous medium and a viscous fluid, *Report No. WFW 91.071*, August 1991, Eindhoven University of Technology.

[20] B.H. Venna, Effect of velocity slip and permeability on Micro polar squeeze films, *International Journal of Computer and Mathematical Sciences* **3**(4) (2014), 41 – 50.

[21] N.K. Verma, S. Mishra, S.U. Siddiqui and R.S. Gupta, Effect of slip velocity on blood flow through a catheterized artery, *Applied Mathematics* **2** (2011), 764 – 770, DOI: 10.4236/am.2011.26102.

[22] L. Zhao, C. Marchioli and H.I. Andersson, Slip velocity of rigid fibers in turbulent channel flow, *Physics of Fluids* **26** (2014), 1 – 26, DOI: 10.1063/1.4881942.